Intermuscular coherence analysis in older adults reveals that gait related arm swing drives lower limb muscles via subcortical and cortical pathways.

Joyce B. Weersink [1], Bauke M. de Jong [1], David M. Halliday [2], Natasha M. Maurits [1]

[1] Department of Neurology, University Medical Center Groningen,
University of Groningen, Hanzeplein 1, POB 30.001, Groningen, The Netherlands.
[2] Department of Electronic Engineering & York Biomedical Research Institute,
University of York, York, YO10 5DD, UK

Running title: arm swing drives lower limb muscles
Key words: EMG, coherence analysis, arm swing, gait
Table of contents category: Neuroscience

No. figures: 5
No. tables: 1

Address for correspondence: N.M. Maurits

Department of Neurology, University Medical Center Groningen,

Hanzeplein 1, P. O. Box 30.001, 9700 RB Groningen, The Netherlands.

Phone: 0031.503612400 | E-mail: n.m.maurits@umcg.nl

Key points summary

- Gait related arm swing in humans supports efficient lower limb muscle activation, indicating a neural coupling between the upper and lower limbs during gait.
- Intermuscular coherence analyses of gait related electromyography from upper and lower limbs in twenty healthy participants identified significant coherence in alpha and beta/gamma bands indicating that upper and lower limbs share common subcortical and cortical drivers that coordinate the rhythmic four limb gait pattern.
- Additional directed connectivity analyses revealed that upper limb muscles drive and shape lower limb muscle activity during gait via subcortical and cortical pathways and to a lesser extent vice versa.
- Our results provide a neural underpinning that arm swing may serve as an effective rehabilitation therapy concerning impaired gait in neurological diseases.

Abstract

Human gait benefits from arm swing, as it enhances efficient lower limb muscle activation in healthy participants as well as patients suffering from neurological impairment. The underlying neuronal mechanisms of such coupling between upper and lower limbs remain poorly understood. The aim of the present study was to examine this coupling by intermuscular coherence analysis during gait. Additionally, directed connectivity analysis of this coupling enabled to assess whether gait related arm swing indeed drives lower limb muscles. To that end, electromyography recordings were obtained from four lower limb muscles and two upper limb muscles bilaterally, during gait, of twenty healthy participants (mean age 67 years, SD 6.8). Intermuscular coherence analysis revealed functional coupling between upper and lower limb muscles in the alpha and beta/gamma band during muscle specific periods of the gait cycle. These effects in the alpha and beta/gamma bands point at involvement of subcortical and cortical sources, respectively, that commonly drive the rhythmic four limb gait pattern in an efficiently coordinated fashion. Directed connectivity analysis revealed that upper limb muscles drive and shape lower limb muscle activity during gait via subcortical and cortical pathways and to a lesser extent vice versa. This indicates that gait related arm swing reflects the recruitment of neuronal support for optimizing the cyclic movement pattern of the lower limbs. These findings thus provide a neural underpinning for arm swing to potentially serve as an effective rehabilitation therapy concerning impaired gait in neurological diseases.

1. Introduction

Locomotion of quadrupeds requires coordination between four limbs, where the forelimbs and hindlimbs move at integral frequencies (Wannier *et al.*, 2001). Human bipedal gait similarly exhibits a characteristic four limb pattern with anti-phase arm swing in the same frequency as the lower limb oscillations, as if they originate from a 'hard-wired' organization within the central nervous system, representing a remnant of neural connections used in quadrupedal gait (Dietz, 2002). This multi-limb coordination has its origin at spinal, subcortical and cortical levels. At spinal level, central pattern generators (CPG) generate tightly-coupled patterns of neural activity that drive stereotyped motor behaviours including gait (Klarner & Zehr, 2018). Propriospinal pathways interconnect these CPGs from cervical and lumbar levels that control the individual limbs, providing an important contribution in generating coordinated interlimb movements (Gernandt & Megirian, 1961; Forssberg *et al.*, 1980; Meinck & Piesiur-Strehlow, 1981; Cazalets & Bertrand, 2000). These pathways modify their activity in cooperation with descending signals from higher order regulation at subcortical and cortical level (Grillner *et al.*, 1995; Debaere *et al.*, 2001; Barthelemy & Nielsen, 2010; Lacquaniti *et al.*, 2012; Takakusaki, 2013).

Although the role of the stereotypical arm movements in human bipedal gait is not as obvious as in quadrupedal gait, they are suggested to be more than just a remnant of quadrupedal gait. Gait related arm swing contributes to stabilization (Hof, 2007; Ortega *et al.*, 2008), energetic efficiency (Ortega *et al.*, 2008; Umberger, 2008; Yizhar *et al.*, 2009) and it is also thought to evoke neuronal support for maintaining the cyclic motor pattern (Massaad *et al.*, 2014; Weersink *et al.*, 2019). This is confirmed by previous studies where adding upper limb movements to lower limb movements during rhythmic tasks improved lower limb muscle recruitment in healthy participants (Huang & Ferris, 2004, 2009; Kao & Ferris, 2005; De Kam *et al.*, 2013; Ogawa *et al.*, 2015) and neurologically impaired patients, such as patients with Parkinson's Disease (Weersink *et al.*, 2018, 2020), stroke (Zehr *et al.*, 2012) or spinal cord injury (de Kam *et al.*, 2013). Patients with incomplete spinal cord injury and spastic paresis also displayed more efficient lower limb muscle activation when stepping with partial body weight support from a harness, i.e. where upper limbs could also move freely, compared to stepping

with support from parallel bars (Visintin & Barbeau, 1994; Behrman & Harkema, 2000). In line with this finding, passively imposed arm swing in incomplete spinal cord injury patients improved muscle activation patterns compared to a resting arms condition (Kawashima *et al.*, 2008). These results suggest that the upper and lower limb muscles are not only coupled by a common neural input, but that the upper limb muscles additionally drive lower limb muscles via a directional neural connection in which the corticospinal pathway might also be involved (Lacquaniti *et al.*, 2012; Takakusaki, 2013).

While electromyography (EMG), in general, enables the assessment of muscle activity implied in distinct movements, coherence and directed connectivity analysis of EMG recordings can be used to explore the neural link between the upper and lower limb muscles during gait and its directionality. EMG detects the electrical potentials generated by muscle cells when activated by a motor neuron, together forming a motor-unit. Such motor-units need to synchronize their firing patterns to smoothly contract the entire muscle, which requires a common presynaptic drive to these motoneurons. Coherence analysis of this motor-unit firing behaviour, expressed in EMG activity, provides information about the organization of these presynaptic drives (Farmer *et al.*, 1993, 1997; Halliday *et al.*, 1995). During locomotion multiple muscles need to collaborate and contract at exact predetermined periods of the gait cycle, which requires additional synchronization between these muscles. Such synchronization has indeed been identified in the pattern of intermuscular coherence between leg muscles during gait, confirming the presence of a common presynaptic drive for this lower limb muscle activity (Grasso *et al.*, 1998; Halliday *et al.*, 2003). An equivalent synchronization between upper and lower limb muscles during gait has not yet been reported. Unfortunately, coherence analysis cannot distinguish directed connections between two muscles from two muscles receiving input from a common driver. Directed connectivity analysis, however, does enable such distinction and may establish directionality or causal effects between two signals (Halliday, 2015). This analysis can thus be used to identify a common driver to both upper and lower limb muscles and test whether upper limb muscles indeed drive the lower limb muscles during gait and/or vice versa.

Commonly studied frequency bands in these analyses include alpha (8-15 Hz), beta (15-30 Hz) and gamma (30-60 Hz) bands as coherence in these bands is argued to

originate from distinct neural origins (Hu *et al.*, 2018; Jensen *et al.*, 2018; Nojima *et al.*, 2018). Intermuscular alpha band coherence is thought to be of subcortical origin as these muscular alpha oscillations are generally not synchronized with cortical activity (Conway *et al.*, 1995; Salenius *et al.*, 1997; Baker & Baker, 2003). Although its exact origin is an issue of ongoing debate, the alpha band especially reflects the involvement of the reticulospinal pathway, which primary responsibility is locomotion control (Grosse & Brown, 2003). Synchronization between the cortex and muscles has been reported especially in the beta band, suggesting this band to be strongly related to the corticospinal drive (Conway *et al.*, 1995; Mima *et al.*, 2000; Fisher *et al.*, 2012; Gwin & Ferris, 2012). Indeed, intermuscular beta band coherence can be used to detect cortical excitability changes following transcranial direct stimulation of the sensorimotor cortex (Power *et al.*, 2006), confirming that intermuscular beta coherence reveals the presence of a shared neural presynaptic input from the higher CNS and particularly from the motor cortex. Finally, intermuscular coherence in the gamma frequency band is also proposed to result from cortical-originating signals and is thought have functional importance in efferent motor commands (Brown *et al.*, 1998; Mima *et al.*, 2000; Clark *et al.*, 2013).

In the present study, we examined the presence of a neural coupling between the upper and lower limb muscles during human gait and explored the temporal characteristics of recorded activity, linked to potential neural substrates. Secondly, we examined the directionality of this neural coupling to determine whether gait related arm swing indeed drives the lower limb muscles. We hypothesized that gait related arm swing can drive lower limbs during gait via both subcortical and cortical pathways. Therefore, coherence and directed connectivity analyses were performed on ambulant EMG from four lower limb muscles and two upper limb muscles involved in the cyclic four-limb walking pattern. To explore the possible neural substrates of these couplings, coherence and connectivity values were evaluated over predetermined frequency bands that are associated with distinct neural origins. Improved understanding of this interlimb coupling during gait and its direction may serve rehabilitation concepts concerning impaired walking in neurological conditions such as Parkinsons disease, spinal cord injury and stroke.

2. Methods

2.1 Ethical approval

The study was executed according to the Declaration of Helsinki (2013), except for registration in a database, and was approved by the ethical committee of the University Medical Center Groningen (reference number: METc 2018/248). Each participant provided written informed consent to the study following verbal and written explanations of the study procedures.

2.2 Participants

Twenty healthy participants (10 males and 10 females, mean age 67 years, SD 6.8 years) were included in the study. Their advanced age enabled future reference with patients suffering from neurodegenerative diseases such as Parkinson's disease. Participants had no neurological disorder or cognitive problems and were right handed according to the Annett Handedness scale (Annett, 1970).

2.3 Task and experimental set-up

In this experiment, participants walked overground at their own comfortable speed through a 150 m hallway in a straight line from start to finish and back. Paired bipolar surface Ag-AgCl EMG electrodes were placed bilaterally on four lower limb muscles, i.e. tibialis anterior, soleus, rectus femoris and biceps femoris, and bilaterally on two shoulder muscles, i.e. deltoideus anterior and deltoideus posterior. Locations of EMG electrodes were according to the SENIAM (https://www.seniam.org) guidelines, where bipolar pairs were oriented parallel to the muscle fibres with an interelectrode distance of 20 mm. However, one always needs to be attentive for the possibility of crosstalk from other muscles when interpreting surface EMG activity (Nene *et al.*, 2004). To detect the moments of heel strike and toe-off, tri-axial accelerometers (Compumedics Neuroscan, Singen, Germany) were placed on the medial side of both ankles and over the L3 lumbar spine segment, using Velcro straps. For the trunk accelerometer, orientation of the three accelerometer axes, X,Y, and Z, when standing in the anatomical position, was medial/lateral, superior/inferior and anterior/posterior, respectively. The EMG and accelerometer signals were recorded at a sampling rate of 512 Hz using a portable amplifier (Siesta, Compumedics Neuroscan, Singen, Germany)

and sent via WIFI to Profusion software (v. 5.0, Compumedics Neuroscan, Singen, Germany) on a laptop for later analysis.

2.4 Accelerometer analysis

Exact time-points of heel strike and toe-off were determined by an approach introduced by Sejdic et al. (2016), described in more detail by Weersink et al. (2019). These time-points were used to calculate stride time and served as a marker for EMG analysis.

2.5 EMG data pre-processing and analysis

EMG data were pre-processed and analysed using custom made scripts in MATLAB 2018a (The Mathworks, Inc., Natick, Massachusetts, United States). To focus on continuous walking, the initial and last five steps and the turning process were removed from the raw EMG data. Subsequently, the data was high pass filtered (5 Hz) using a finite impulse response filter, corrected for the delay introduced by the filter and full-wave rectified. Single trial envelopes were calculated for the filtered and rectified EMG activity and time warped to the individual stride time using linear interpolation. After time-warping, individual EMG envelopes were expressed as percentage of the mean activity of that individual during one gait cycle. Resulting EMG envelopes were subsequently smoothed using a 10 ms moving average window, pooled and plotted.

The time dependent intermuscular coherence analysis was based on a unified framework developed by Halliday et al. (1995), which allowed the correlation between EMG signals of the shoulders and the legs to be characterized as a function of time and frequency. A sliding window of 200 ms was used to generate periodograms for 22 offsets relative to right heel strike with an interval of 50 ms. This resulted in an overall analysis window of 1100 ms, which is equal to the average stride time over all subjects. As individual stride times were comparable between subjects (mean 1.09 sec, SD 0.06), time-normalization was not applied. Averaging these periodograms for each offset across all gait cycles was used to construct estimates of spectra, where $f_{xx}(\lambda)$ and $f_{yy}(\lambda)$ represent the autospectra of processes x and y, respectively. The cross-spectrum between x and y is denoted by $f_{yx}(\lambda)$ and is estimated in a similar manner. The coherence function between the two signals at frequency λ is defined as:

$$|R_{yx}(\lambda)|^2 = \frac{|f_{yx}(\lambda)|^2}{f_{xx}(\lambda) f_{yy(\lambda)}}.$$

This provides a normalised measure of correlation in the frequency domain which ranges from 0 to 1. Coherence was calculated for frequencies up to 70 Hz and for the previously mentioned offsets. Combining these 22 offsets results in an individual heat map showing time-dependent coherence between two signals for distinct frequencies during the gait cycle relative to the time of heel strike. These individual time-dependent coherence estimates were pooled to produce a group estimate. Subsequently, significant ($p < 0.05$) coherence estimates were determined and plotted in heat maps (Halliday *et al.*, 1995).

Estimates of directed connectivity were computed using a non-parametric directionality (NPD) analysis, which is a framework that decomposes classical, nonparametric Fourier-based coherence estimates by direction and is described in more detail in Halliday (2015). In short, in this approach optimal whitening or minimum mean square error (MMSE) whitening is used for prewhitening of the two EMG signals. Pre-whitening refers to the process of filtering a signal before spectral analysis to make its frequency content closer to white noise. This generates two new random processes that have spectra equal to 1 at all frequencies and that have the same coherence as the two original signals. As the autospectra for these, denoted as $f_{xx}^{w}(\lambda)$, $f_{yy}^{w}(\lambda)$, then become equal to 1, only the cross-spectrum from these pre-whitened processes is used to calculate the coherence, which is then identical to the original coherence: $\left|R_{yx}^{w}(\lambda)\right|^2 = \left|f_{yx}^{w}(\lambda)\right|^2 = \left|R_{yx}(\lambda)\right|^2$. Subsequently, an inverse Fourier transform is used to produce a time domain correlation measure from this prewhitened cross-spectrum as

$$\rho_{yx}(\tau) = \frac{1}{2\pi}\int_{-\pi}^{\pi} f_{yx}^{w}(\lambda)\, e^{i\lambda t} d\lambda .$$

The difference with the standard approach to generate a cross-covariance estimate in the time domain is that the prewhitened time domain correlation measure $\rho_{yx}(\tau)$ only has features that occur as a result of the correlation between the signals. This allows effective removal of the confounding influence of the original signals' autocorrelation. From the resulting time domain correlation measure, three quantities are extracted according to time lag i.e. components with a negative time lag, $\tau < 0$, the value at zero time lag, $\tau = 0$, and components at positive time lags, $\tau > 0$. Three inverse Fourier

transforms over these three lag ranges are then used to obtain the reverse, zero-lag and forward components of coherence, respectively, as

$$\left|R_{yx}(\lambda)\right|^2 = \left|R'_{yx;-}(\lambda)\right|^2 + \left|R'_{yx;0}(\lambda)\right|^2 + \left|R'_{yx;+}(\lambda)\right|^2,$$

where the prime indicates frequency domain quantities calculated from a subset of time lags in $\rho_{yx}(\tau)$, and the symbols $-, +, 0$ indicate the reverse, zero lag and forward components of coherence, respectively. These three components provide a summative decomposition of the original nonparametric coherence at each frequency into reverse, zero-lag and forward components. The correlation values for corresponding time lags were subsequently pooled and plotted. When interpreting these time domain estimates, time lags larger than 70 ms were considered to correspond to transcortical pathways (Nielsen *et al.*, 1997) while time lags smaller than 70 ms were considered to correspond to subcortical pathways. As the action potentials have to travel a longer distance to the lower limb muscles compared to the upper limb muscles, there might be a conduction delay up to approximately 7 ms (Matamala *et al.*, 2013). Therefore, time lags smaller than 7 ms in the time domain correlation plots were disregarded as they could be due to this distance related delay.

Both time-dependent coherence analysis and non-parametric directionality analysis were performed for all shoulder-leg combinations, resulting in 32 combinations in each of the 20 participants. Leg-leg and shoulder-shoulder combinations were not examined as they were beyond the scope of the current study. In locomotor data, the periodicity of the gait cycle dominates the low-frequency spectral components (<8 Hz) of EMG data, and therefore these frequencies were disregarded.

2.6 Statistical analysis

MATLAB 2018a (The Mathworks, Inc., Natick, Massachusetts, United States) was used for statistical testing of the connectivity estimates for each muscle combination. To compare the forward and reverse connectivity a Wilcoxon Signed Rank test was performed for the area under the curve for the alpha (8-12Hz), beta (12-30Hz) and gamma (30-60 Hz) frequency bands. All p-values were corrected for multiple

comparisons using the Benjamini Hochberg false discovery rate (Benjamini and Hochberg 1995; Benjamini and Yekutielie 2001). For all statistical tests an alpha level of 0.05 was assumed.

3. Results

3.1 Time-dependent coherence

Although significant intermuscular coherence occurred in all 32 pairs of shoulder and leg muscles (Fig. 1), highest coherence values were found between shoulder muscles (deltoideus anterior and posterior) and proximal leg muscles (biceps femoris and rectus femoris). Significant alpha (8-15 Hz) coherence occurred during the major part of the gait cycle with its peak values during more distinct periods of the gait cycle and is per muscle described in more detail below. Periods of highest alpha coherence co-occurred with periods of high beta and gamma coherence in frequencies ranging from 15 to 50 Hz. Both left and right biceps femoris muscles had these high coherence values with the shoulder muscles during the middle to end of their stance phases. For these muscle pairs, lowest coherence was found for ipsilateral left side and highest coherence for ipsilateral right side. Rectus femoris muscles exhibited significant coherence with the shoulder muscles during the end of the stance phase and during the swing phase, with a reduction in coherence around the time of toe-off and heel strike. For these muscle pairs, highest coherence was found between the right shoulder muscles and left rectus femoris muscle, (i.e. in a diagonal fashion). For the distal leg muscles these periods of significant coherence with the shoulder muscles are less pronounced and more dispersed. Significant coherence between bilateral soleus muscles and bilateral shoulder muscles was generally found during middle swing phase up until early stance phase. Coherence between the bilateral tibialis anterior muscles and bilateral shoulder muscles was also more dispersed but was found, especially, during the end of the stance phase and beginning of the swing phase and this was more pronounced for the right leg.

Overall, moments of highest coherence between shoulder and leg muscles corresponded with the less active phase of the involved leg muscle, according to the average EMG envelopes for each independent muscle that are depicted in Fig 2.

3.2 Time domain estimates of coherence

This coherence between the upper and lower limbs can be transformed to the time domain (Fig 3A), which then shows whether the coherent shoulder and leg muscle signals are completely synchronized or whether one signal precedes or follows the

other. These time domain estimates can be decomposed into three components. First, if the signals from the shoulder and leg muscles were completely synchronized in the time domain a peak around 0 ms was observed, which points at a common driver to both shoulder and leg muscles. Significant peaks around 0 ms were most pronounced between the bilateral shoulder muscles and proximal leg muscles. Significant peaks around 0 ms were also observed between the right shoulder muscles and left soleus and right tibialis anterior muscle and between left shoulder muscles and right soleus muscle. Secondly, signals from the shoulder muscles that preceded the signals from the leg muscles were depicted in the time domain estimates by significant peaks with a positive time lag, which suggests that the shoulder muscles drive the leg muscles. These positive time lags can be divided into intervals corresponding to conduction times of either subcortical or cortical pathways and are suggested to point at the involvement of these pathways for this drive (Fig 3B). Significant positive time lags corresponding with conduction times of subcortical pathways (7 until 70 ms) were observed between bilateral shoulder muscles and proximal leg and right tibialis anterior muscles. Significant positive time lags corresponding with conduction times of transcortical pathways (> 70 ms) were found between bilateral shoulder muscles and bilateral biceps femoris and right rectus femoris muscles. Significant positive time lags related to transcortical pathways were additionally found between the left shoulder muscles and right soleus muscle and between the right shoulder muscles and left rectus femoris muscle and right tibialis anterior muscle. Thirdly, signals from shoulder muscles that lagged signals from the leg muscles were depicted in the time domain estimates as significant peaks with negative time lags, which suggests that leg muscles can also drive the shoulder muscles. These negative time lags could again be divided into intervals corresponding to conduction times of subcortical and transcortical pathways. Significant negative time lags related to conduction times of subcortical pathways (-7 ms until -70 ms) were found between bilateral proximal leg muscles and bilateral shoulder muscles, between bilateral distal leg muscles and right shoulders muscles and between right tibialis anterior muscle and left shoulder muscles. Significant negative time lags corresponding to conduction times of transcortical pathways (< -70 ms) were particularly found between left proximal leg muscles and bilateral shoulder muscles,

right biceps femoris and left shoulder muscles, right rectus femoris and right shoulder muscles and between right tibialis anterior and bilateral shoulder muscles.

3.3 Zero-lag component of coherence

Coherence is the frequency domain equivalent of these time estimates and the total coherence between shoulder and leg muscles can be decomposed into the previously described three time domain components, i.e. the zero-lag, positive and negative time lag components. Coherence estimates from the zero lag component are shown in Fig. 4 and point at a common pre-synaptic input from a common driver to these muscles. Here, alpha band coherence suggests input from subcortical pathways and beta/gamma band coherence suggests cortical input. For frequencies in the alpha band, zero-lag components were found for all pairs of shoulder muscles and proximal leg muscles, with highest values between biceps femoris of the right leg and bilateral shoulder muscles and between the left rectus femoris muscle and right shoulder muscles. Also for frequencies in the beta (15-30 Hz) band, all pairs of proximal leg muscles and shoulder muscles displayed zero-lag components. Highest connectivity measures for frequencies in this band were also found between the biceps femoris muscle of the right leg and bilateral shoulder muscles and between the left rectus femoris muscle and right shoulder muscles. In the gamma band, all proximal leg muscles displayed zero-lag connectivity with bilateral shoulder muscles, where only low values were observed between distal leg muscles and bilateral shoulder muscles.

3.4 Forward and reverse directed components of coherence

Coherence estimates from the components of the positive and negative time lag, which were respectively coined the forward directed component and reverse directed component, are shown in Fig. 5 (together with statistical significance levels). Coherence in the forward directed components would mean that these shoulder muscle signals lead the leg muscle signals suggesting that the shoulder muscles drove the leg muscles. In contrast, significant coherence for the reverse directed components means that signals from the shoulder muscles lagged the signals from the leg muscles, suggesting that leg muscles could drive the shoulder muscles too. In the subcortical alpha band, bilateral shoulder muscles were found to drive bilateral proximal leg muscles and right distal leg muscles. Vice versa, bilateral proximal leg muscles and the right tibialis anterior muscle

drove the bilateral shoulder muscles too, for frequencies in this band. For (cortical) beta frequencies, only right shoulder muscles were found to drive bilateral proximal leg muscles and the right tibialis anterior muscle. Conversely, left rectus femoris muscle and right biceps femoris muscle drove bilateral shoulder muscles for these frequencies. In the gamma band, especially for frequencies below 45 Hz, right shoulder muscles drove the right tibialis anterior muscle and bilateral proximal leg muscles, with highest values for the right biceps femoris muscle. For this frequency band, minimal drive from leg muscles to shoulder muscles was observed during gait.

To statistically test whether the shoulder muscles drove the leg muscles more than vice versa, coherence estimates from the alpha, beta and gamma frequency band for the forward directed component were compared to those for the reverse directed component. When there was a significant difference between the two components in these frequency bands, corresponding p-values were noted in the right upper corner of the plot of that muscle combination in Fig. 5. In 20 out of 21 significant differences, forward directed connectivity was enhanced compared to reverse directed connectivity, implicating that for these pairs shoulder muscles drove leg muscles more than vice versa. Only the right rectus femoris muscle drove the left deltoideus anterior muscle (median 0.108, IQ 0.207) significantly more ($p = 0.028$, $n = 20$ participants) than vice versa (median 0.093, IQ 0.103) in the gamma band. The majority (18/20) of these significantly stronger forward directed connectivities involved the right shoulder muscles driving the leg muscles in the alpha (9/20) and beta (8/20) band. Details on statistical significance concerning all muscle pairs are provided in Table 1.

4. Discussion

In the present study, we found intermuscular coherence between shoulder and leg muscles in the alpha and beta/gamma band during gait. Such coherence in specifically the alpha and beta/gamma bands provides arguments for a neural coupling between upper and lower limbs derived from respectively a subcortical and cortical origin, which was also consistent with time estimates corresponding to conduction times of these pathways. This coupling consisted of shoulder muscles driving the leg muscles and to a lesser extent also vice versa, besides input from a common driver to these muscles. These observations support the idea that gait related arm swing is the expression of neuronal support for lower limb movements during gait.

Such intermuscular coherence reflects synchronized motor unit activity and is commonly observed in synergistic muscles that act together to accomplish a single joint movement (De Luca & Erim, 2002; Laine *et al.*, 2015). However, intermuscular coherence has also been observed between muscles acting on distinct joints such as during bilateral movements (Boonstra *et al.*, 2007, 2009) and whole-body tasks (Boonstra & Breakspear, 2012; Danna-Dos-Santos *et al.*, 2014; Kerkman *et al.*, 2017), suggesting that the central nervous system also uses common neural inputs to assemble these larger functional units. Our present study also reports intermuscular coherence between shoulder and leg muscles during distinct periods of the gait cycle, indicating that these muscles are included in a gait related functional unit employing neural coupling. Interestingly, the coupling was particularly present between shoulder and proximal leg muscles suggesting that there is a stronger coupling with proximal than with distal leg muscles, which has also been previously suggested (Sylos-Labini *et al.*, 2014). Such interlimb coupling during motor tasks arises from different neural origins and it is generally acknowledged that intermuscular alpha band coherence primarily reflects coupling via subcortical interconnections (Conway *et al.*, 1995; Salenius *et al.*, 1997; Baker & Baker, 2003) while beta/gamma band coherence reflects the involvement of particularly transcortical pathways (Conway *et al.*, 1995; Mima *et al.*, 2000; Fisher *et al.*, 2012). This was also observed in our study, where muscle combinations with directed connectivity in alpha and beta/gamma frequency bands indeed also exhibited significant time lags that are compatible with conduction times of subcortical and

transcortical pathways, respectively. In the following text, coherence in alpha and beta/gamma frequency bands will be referred to as cortical and subcortical pathways, although it should be acknowledged that coherence in these frequency bands does not solely arise from coupling via these pathways.

The observed neural coupling can be divided into three directional factors depending on the temporal relationship between signals, where a zero time interval reflects a common driver to both shoulder and leg muscles. Such a common driver particularly enables efficient multi-limb coordination during gait and in our study the zero lag component was a relatively large contributor to the observed total coherence. We found markers for subcortical (i.e. alpha) and cortical (i.e. beta/gamma) sources that commonly drive bilateral shoulder and proximal leg muscles. This subcortical driver is thought to mainly reflect coupling via the reticulospinal pathway, as this pathway plays a pivotal role in gait control by sending locomotor commands to spinal interneuronal circuits, eventually controlling CPG activity that drives the rhythmic four limb pattern (Grosse & Brown, 2003; Matsuyama *et al.*, 2004). The sharp peak around 0 ms observed in the time estimates might be a reflection of this synchronized CPG activity. In addition, due to the role of arm swing in maintaining the body's equilibrium during gait, coupling via the vestibular pathway may also contribute to this common subcortical driver. At cortical level, previous studies have reported that the motor cortex contributes to gait related upper limb muscle activity (Barthelemy & Nielsen, 2010) as well as lower limb muscle activity (Petersen *et al.*, 2012). Our study is the first to report that these four limbs share a *common* cortical driver during gait, which could contribute to the coordination and synchronization of these simultaneous upper and lower limb movements during gait. When interpreting the zero-lag components, it is important to keep in mind that some of the actual zero lag components are not captured in the ~2 ms wide bin due to conduction delays.

In the remaining two directions that constitute this neural coupling, upper limb muscles can drive or modulate lower limb muscles and vice versa. This bidirectional coupling was identified on a subcortical level (i.e. alpha) for bilateral shoulder muscles and leg muscles, and on a cortical (i.e. beta/gamma) level for muscle pairs including only the right shoulder muscles. One might speculate that the latter could be explained by the fact that all participants were right handed and that this handedness is also reflected by a

similar arm dominance during gait. In line with this, the origin of handedness is mostly embedded in cortical pathways (Hammond, 2002), which might explain why these left-right differences are solely shown on a cortical level. As the right shoulder muscles drive bilateral leg muscles, the cortical coupling of upper and lower limbs occurs within and between hemispheres for which transcallosal connections are required. The supplementary motor area is a midline cortical area located anterior of the primary motor cortex, which has strong and widespread connections with the motor field of the contralateral cortex and is therefore also a good candidate for the cortical source involved in this interlimb coupling during gait (Rouiller *et al.*, 1994; Ruddy *et al.*, 2017). The presently observed directional coupling between shoulder and leg muscles is in line with previous reports of rhythmic upper limb movements affecting reflex responses in lower limb movements (Cerri *et al.*, 2003; Frigon *et al.*, 2004; Palomino *et al.*, 2011; Massaad *et al.*, 2014) and provides a neural underpinning for previous observations that the addition of upper limb movements to lower limb movements during rhythmic movement did improve lower limb muscle recruitment in healthy participants (Jakobi & Chilibeck, 2001; Huang & Ferris, 2004, 2009; Kao & Ferris, 2005; De Kam *et al.*, 2013) and neurologically impaired patients (Zehr *et al.*, 2012; de Kam *et al.*, 2013; Weersink *et al.*, 2020). On both subcortical (i.e. alpha) and cortical (i.e. beta/gamma) levels, shoulder muscles were found to significantly drive leg muscles more than vice versa, explaining why in a previous study arm movements had more influence on leg EMG than leg movements had on arm EMG (Huang & Ferris, 2009). Interestingly, this is the opposite direction compared to that observed in quadrupedal gait in rats and cats, where caudorostral connections between the CPGs appeared to be most powerful (Juvin *et al.*, 2005; Akay & Büschges, 2006). A previous human experiment, applying combined leg and arm cycling tasks, showed that changing the leg cycling frequency affected the cadence of arm cycling while changing the frequency of arm cycling did not affect the leg cycling cadence (Sakamoto *et al.*, 2014). The results of this double task may underscore de natural dominance of a cyclic movement pattern of the legs in gait but did, however, not address the coherence of four-limb control in actual human gait. Quadrupedal gait usually takes the form of an in-phase synchronization between diagonal front and hind limbs and, at higher speed, the nervous system naturally prefers in-phase over the more complex anti-phase

movements. Consistently, intraspinal interconnections between cervical and lumbar CPGs in rats were found to also favour this diagonal coupling (Juvin *et al.*, 2005, 2007). The current study confirms the presence of such a diagonal coupling between upper and lower limb muscles during human bipedal gait, although ipsilateral coupling between upper and lower limbs was observed as well. This ipsilateral coupling in humans was also observed by Huang & Ferris (2009), who attributed this finding to a coupled corticospinal drive that, in their maximal effort task, was proposed to be more dominant than spinal mechanisms, which favour diagonal coupling. The combined diagonal and ipsilateral coupling of the upper and lower limbs in our study may thus support the inference of a concerted involvement of spinal and corticospinal pathways in this neural interlimb coupling during gait.

Although the exact mechanism and function of this directional coupling between shoulder and leg muscles is unknown, it is proposed that the shoulder muscle activity optimizes lower limb locomotive muscle activity (Huang & Ferris, 2004; Kao & Ferris, 2005). In our study, subcortical coupling (i.e. alpha) was present during the majority of the gait cycle and was significant in both directions, suggesting that this is a relatively straight-forward mechanism of enhancing CPG activity of the other limbs. This might contribute to the previously reported EMG enhancement in the lower limbs when rhythmic arm movements were performed (Huang & Ferris, 2004; Kao & Ferris, 2005). However, interlimb coupling at cortical level (i.e. beta/gamma) was found to be strongest during the less active stages of the leg muscles. This suggests that the coupled neural input may be a mechanism to constrain the modulation of activity across multiple muscles used in gait. In line with this hypothesis, passively imposed upper limb movements were found to shorten the soleus EMG activity during human gait (Kawashima *et al.*, 2008) and rhythmic upper limb cycling reduced reflexes in lower limb muscles during specific phases of cycling (Frigon *et al.*, 2004; Loadman & Zehr, 2007; Palomino *et al.*, 2011). This indicates that the neural signal that is modulated by the upper limb movements contributes not merely by enhancing but also by shaping the lower limb locomotive muscle activity by eliminating the inappropriate activity.

When interpreting the results, it is important to keep in mind that intermuscular coherence during gait can be dependent on certain circumstances, such as age (dos Santos *et al.*, 2020) or the frequency ratio between arm and leg swing (Kerkman *et al.*,

2020). The latter is found to be dependent on walking speed, where a 1:1 ratio is found during a normal walking speed and a 2:1 ratio during very slow walking (< 0.8 m/s) (Wagenaar & Van Emmerik, 2000). The present study examined older adults with a normal walking speed (mean 1.27 m/s, SD 0.23), which was therefore associated with a 1:1 arm-leg frequency ratio. This 'normal value' thus provides a standard for studying gait disorders in e.g. Parkinson's disease, which generally concerns patients at more advanced age. Moreover, exploring these intermuscular coherences in a younger population and during very slow walking allows translation of the current findings to gait rehabilitation in other neurological diseases.

5. Conclusion

Intermuscular coherence analysis showed that upper and lower limbs are functionally coupled during muscle specific periods of the gait cycle. Involvement of alpha and beta/gamma frequency bands pointed at common subcortical and cortical drivers that may enable efficient coordination of this rhythmic four limb gait pattern. Additionally, upper limb muscles were found to drive and shape lower limb muscle activity during gait via subcortical and cortical pathways and to a lesser extent vice versa. This indicates that gait related arm swing is not merely a remnant of quadrupedal gait, but indeed reflects the recruitment of neuronal support for optimizing the cyclic movement pattern of the lower limbs. This provides a neural underpinning for arm swing to be an effective rehabilitation therapy concerning impaired gait in neurological conditions including Parkinson disease, spinal cord injury and stroke.

References

Akay T & Büschges A (2006). Load signals assist the generation of movement-dependent reflex reversal in the femur-tibia joint of stick insects. *J Neurophysiol* **96,** 3532–3537.

Annett M (1970). A classification of hand preference by association analysis. *Br J Psychol* **61,** 303–321.

Baker MR & Baker SN (2003). The effect of diazepam on motor cortical oscillations and corticomuscular coherence studied in man. *J Physiol* **546,** 931–942.

Barthelemy D & Nielsen JB (2010). Corticospinal contribution to arm muscle activity during human walking. *J Physiol* **588,** 967–979.

Behrman AL & Harkema SJ (2000). Locomotor training after human spinal cord injury : a series of case studies. *Phys Ther Spinal Cord Inj Spec Ser* **80,** 688–700.

Boonstra TW & Breakspear M (2012). Neural mechanisms of intermuscular coherence: Implications for the rectification of surface electromyography. *J Neurophysiol* **107,** 796–807.

Boonstra TW, Daffertshofer A, Van As E, Van Der Vlugt S & Beek PJ (2007). Bilateral motor unit synchronization is functionally organized. *Exp Brain Res* **178,** 79–88.

Boonstra TW, Daffertshofer A, Roerdink M, Flipse I, Groenewoud K & Beek PJ (2009). Bilateral motor unit synchronization of leg muscles during a simple dynamic balance task. *Eur J Neurosci* **29,** 613–622.

Brown P, Salenius S, Rothwell JC & Hari R (1998). Cortical correlate of the piper rhythm in humans. *J Neurophysiol* **80,** 2911–2917.

Cazalets JR & Bertrand S (2000). Coupling between lumbar and sacral motor networks in the neonatal rat spinal cord. *Eur J Neurosci* **12,** 2993–3002.

Cerri G, Borroni P & Baldissera F (2003). Cyclic H-reflex modulation in resting forearm related to contractions of foot movers, not to foot movement. *J Neurophysiol* **90,** 81–88.

Clark DJ, Kautz SA, Bauer AR, Chen YT & Christou EA (2013). Synchronous EMG activity in the piper frequency band reveals the corticospinal demand of walking tasks. *Ann Biomed Eng* **41,** 1778–1786.

Conway BA, Halliday DM, Farmer SF, Shahani U, Maas P, Weir AI & Rosenberg JR (1995). Synchronization between motor cortex and spinal motoneuronal pool during the performance of a maintained motor task in man. *J Physiol* **489,** 917–924.

Danna-Dos-Santos A, Boonstra TW, Degani AM, Cardoso VS, Magalhaes AT, Mochizuki L & Leonard CT (2014). Multi-muscle control during bipedal stance: An EMG-EMG analysis approach. *Exp Brain Res* **232,** 75–87.

Debaere F, Swinnen SP, Be E, Sunaert S, Hecke P Van & Duysens J (2001). Brain Areas Involved in Interlimb Coordination : A Distributed Network. *Neuroimage* **14,** 947–958.

Dietz V (2002). Do human bipeds use quadrupedal coordination? *Trends Neurosci* **25,** 462–467.

Farmer S, Bremner F, Halliday D, Rosenberg J & Stephens J (1993). the Frequency Content of Common Synaptic Inputs To Motoneurones studied during voluntary isometric contraction in man. *J Physiol* **470,** 127–155.

Farmer SF, Halliday DM, Conway BA, Stephens JA & Rosenberg JR (1997). A review of recent applications of cross-correlation methodologies to human motor unit recording. *J Neurosci Methods* **74,** 175–187.

Fisher KM, Zaaimi B, Williams TL, Baker SN & Baker MR (2012). Beta-band intermuscular coherence: A novel biomarker of upper motor neuron dysfunction in motor neuron disease. *Brain* **135,** 2849–2864.

Forssberg H, Grillner S, Halbertsma J & Rossignol S (1980). The locomotion of the low spinal cat. II. Interlimb coordination. *Acta Physiol Scand* **108,** 283–295.

Frigon A, Collins DF & Zehr EP (2004). Effect of Rhythmic Arm Movement on Reflexes in the Legs: Modulation of Soleus H-Reflexes and Somatosensory Conditioning. *J Neurophysiol* **91,** 1516–1523.

Gernandt B & Megirian D (1961). Ascending propriospinal mechanisms. *J Neurophysiol* **24,** 364–376.

Grasso R, Bianchi L & Lacquaniti F (1998). Motor patterns for human gait: Backward versus forward locomotion. *J Neurophysiol* **80,** 1868–1885.

Grillner S, Deliagina T, El Manira A, Hill RH, Orlovsky GN, Wallén P, Ekeberg Ö & Lansner A (1995). Neural networks that co-ordinate locomotion and body orientation in lamprey. *Trends Neurosci* **18,** 270–279.

Grosse P & Brown P (2003). Acoustic startle evokes bilaterally synchronous oscillatory EMG activity in the healthy human. *J Neurophysiol* **90,** 1654–1661.

Gwin JT & Ferris DP (2012). Beta- and gamma range human lower limb corticomuscular coherence. *Front Hum Neurosci* **6,** 1–6.

Halliday D (2015). Non-parametric directionality measures for time series and point process data. *J Integr Neurosci* **14,** 253–277.

Halliday D, Conway B, Christensen L, Hansen N, Petersen N & Nielsen J (2003). Functional coupling of motor units is modulated during walking in human subjects. *J Neurophysiol* **89,** 960–968.

Halliday DM, Rosenberg JR, Amjad AM, Breeze P, Conway BA & Farmer SF (1995). A framework for the analysis of mixed time series/point process data - theory and application to the study of physiological tremor, single motor unit discharges and electromyograms. *Prog Biophys Mol Biol* **64,** 237–278.

Hammond G (2002). Correlates of human handedness in primary motor cortex: A review and hypothesis. *Neurosci Biobehav Rev* **26,** 285–292.

Hof AL (2007). The equations of motion for a standing human reveal three mechanisms for balance. *J Biomech* **40,** 451–457.

Hu G, Yang W, Chen X, Qi W, Li X, Du Y & Xie P (2018). Estimation of time-varying coherence amongst synergistic muscles during wrist movements. *Front Neurosci* **12,** 1–12.

Huang H & Ferris D (2004). Neural coupling between upper and lower limbs during

recumbent stepping. *J Appl Physiol* **97,** 1299–1308.

Huang H & Ferris D (2009). Upper and Lower Limb Muscle Activation Is Bidirectionally and Ipsilaterally Coupled. *Med Sci Sport Exerc* **41,** 1778–1789.

Jakobi J & Chilibeck P (2001). Bilateral and Unilateral Contractions: Possible Differences in Maximal Voluntary Force. *Can J Appl Physiol* **26,** 12–33.

Jensen P, Jensen NJ, Terkildsen CU, Choi JT, Nielsen JB & Geertsen SS (2018). Increased central common drive to ankle plantar flexor and dorsiflexor muscles during visually guided gait. *Physiol Rep* **6,** 1–11.

Juvin L, Simmers J & Morin D (2005). Propriospinal circuitry underlying interlimb coordination in mammalian quadrupedal locomotion. *J Neurosci* **25,** 6025–6035.

Juvin L, Simmers J & Morin D (2007). Locomotor rhythmogenesis in the isolated rat spinal cord: A phase-coupled set of symmetrical flexion-extension oscillators. *J Physiol* **583,** 115–128.

de Kam D, Duysens J & Dietz V (2013). Do we need allowing arm movements for rehabilitation of gait? In *Converging clinical and engineering research on neurorehabilitation by J.L. Pons et al.*, pp. 957–961.

De Kam D, Rijken H, Manintveld T, Nienhuis B, Dietz V & Duysens J (2013). Arm movements can increase leg muscle activity during submaximal recumbent stepping in neurologically intact individuals. *J Appl Physiol* **115,** 34–42.

Kao PC & Ferris DP (2005). The effect of movement frequency on interlimb coupling during recumbent stepping. *Motor Control* **9,** 144–163.

Kawashima N, Nozaki D, Abe MO & Nakazawa K (2008). Shaping appropriate locomotive motor output through interlimb neural pathway within spinal cord in humans. *J Neurophysiol* **99,** 2946–2955.

Kerkman JN, Bekius A, Boonstra TW, Daffertshofer A & Dominici N (2020). Muscle Synergies and Coherence Networks Reflect Different Modes of Coordination During Walking. *Front Physiol* **11,** 1–13.

Kerkman JN, Daffertshofer A, Gollo LL, Breakspear M & Boonstra TW (2017).

Functional connectivity analysis of multiplex muscle network across frequencies. *Proc Annu Int Conf IEEE Eng Med Biol Soc*1567–1570.

Klarner T & Zehr EP (2018). Sherlock Holmes and the curious case of the human locomotor central pattern generator. *J Neurophysiol* **120,** 53–77.

Lacquaniti F, Ivanenko YP & Zago M (2012). Patterned control of human locomotion. *J Physiol* **590,** 2189–2199.

Laine CM, Martinez-Valdes E, Falla D, Mayer F & Farina D (2015). Motor neuron pools of synergistic thigh muscles share most of their synaptic input. *J Neurosci* **35,** 12207–12216.

Loadman PM & Zehr EP (2007). Rhythmic arm cycling produces a non-specific signal that suppresses Soleus H-reflex amplitude in stationary legs. *Exp Brain Res* **179,** 199–208.

De Luca CJ & Erim Z (2002). Common drive in motor units of a synergistic muscle pair. *J Neurophysiol* **87,** 2200–2204.

Massaad F, Levin O, Meyns P, Drijkoningen D, Swinnen S & Duysens J (2014). Arm sway holds sway: Locomotor-like modulation of leg reflexes when arms swing in alternation. *Neuroscience* **258,** 34–46.

Matamala JM, Núñez C, Lera L, Verdugo RJ, Sánchez H, Albala C & Castillo JL (2013). Motor evoked potentials by transcranial magnetic stimulation in healthy elderly people. *Somatosens Mot Res* **30,** 201–205.

Matsuyama K, Mori F, Nakajima K, Drew T, Aoki M & Mori S (2004). Locomotor role of the corticoreticular-reticulospinal-spinal interneuronal system. *Prog Brain Res* **143,** 239–249.

Meinck HM & Piesiur-Strehlow B (1981). Reflexes evoked in leg muscles from arm afferents: A propriospinal pathway in man? *Exp Brain Res* **43,** 78–86.

Mima T, Steger J, Schulman AE, Gerloff C & Hallett M (2000). Electroencephalographic measurement of motor cortex control of muscle activity in humans. *Clin Neurophysiol* **111,** 326–337.

Nene A, Byrne C & Hermens H (2004). Is rectus femoris really a part of quadriceps? Assessment of rectus femoris function during gait in able-bodied adults. *Gait Posture* **20,** 1–13.

Nielsen J, Petersen N & Fedirchuk B (1997). Evidence suggesting a transcortical pathway from cutaneous foot afferents to tibialis anterior motoneurones in man. *J Physiol* **501,** 473–484.

Nojima I, Watanabe T, Saito K, Tanabe S & Kanazawa H (2018). Modulation of EMG-EMG coherence in a choice stepping task. *Front Hum Neurosci* **12,** 1–11.

Ogawa T, Sato T, Ogata T, Yamamoto SI, Nakazawa K & Kawashima N (2015). Rhytmic arm swing enhances patterned locomotor-like muscle activity in passively moved lower extremities. *Physiol Rep* **3,** e12317.

Ortega JD, Fehlman LA & Farley CT (2008). Effects of aging and arm swing on the metabolic cost of stability in human walking. *J Biomech* **41,** 3303–3308.

Palomino AF, Hundza SR & Zehr EP (2011). Rhythmic arm cycling differentially modulates stretch and H-reflex amplitudes in soleus muscle. *Exp Brain Res* **214,** 529–537.

Petersen TH, Willerslev-Olsen M, Conway BA & Nielsen JB (2012). Motor cortex drives the muscles during walking in human subjects. *J Physiol* **10,** 2443–2452.

Power HA, Norton JA, Porter CL, Doyle Z, Hui I & Chan KM (2006). Transcranial direct current stimulation of the primary motor cortex affects cortical drive to human musculature as assessed by intermuscular coherence. *J Physiol* **577,** 795–803.

Rouiller EM, Babalian A, Kazennikov O, Moret V, Yu XH & Wiesendanger M (1994). Transcallosal connections of the distal forelimb representations of the primary and supplementary motor cortical areas in macaque monkeys. *Exp Brain Res* **102,** 227–243.

Ruddy KL, Leemans A & Carson RG (2017). Transcallosal connectivity of the human cortical motor network. *Brain Struct Funct* **222,** 1243–1252.

Sakamoto M, Tazoe T, Nakajima T, Endoh T & Komiyama T (2014). Leg automaticity is stronger than arm automaticity during simultaneous arm and leg cycling. *Neurosci Lett* **564,** 62–66.

Salenius S, Portin K, Kajola M, Salmelin R & Hari R (1997). Cortical control of human motoneuron firing during isometric contraction. *J Neurophysiol* **77,** 3401–3405.

dos Santos PCR, Lamoth CJC, Barbieri FA, Zijdewind I, Gobbi LTB & Hortobágyi T (2020). Age-specific modulation of intermuscular beta coherence during gait before and after experimentally induced fatigue. *Sci Rep* **10,** 1–12.

Sejdic E, Lowry KA, Bellanca J, Perera S, Redfern MS & Brach JS (2016). Extraction of Stride Events From Gait Accelerometry During Treadmill Walking. *IEEE J Transl Eng Heal Med* **4,** 1–11.

Sylos-Labini F, Ivanenko YP, MacLellan MJ, Cappellini G, Poppele RE & Lacquaniti F (2014). Locomotor-like leg movements evoked by rhythmic arm movements in humans. *PLoS One*; DOI: 10.1371/journal.pone.0090775.

Takakusaki K (2013). Neurophysiology of gait: From the spinal cord to the frontal lobe. *Mov Disord* **28,** 1483–1491.

Umberger BR (2008). Effects of suppressing arm swing on kinematics, kinetics, and energetics of human walking. *J Biomech* **41,** 2575–2580.

Visintin M & Barbeau H (1994). The effects of parallel bars, body weight support and speed on the modulation of the locomotor pattern of spastic paretic gait. A preliminary communication. *Paraplegia* **32,** 540–553.

Wagenaar RC & Van Emmerik REA (2000). Resonant frequencies of arms and legs identify different walking patterns. *J Biomech* **33,** 853–861.

Wannier T, Bastiaanse C, Colombo G & Dietz V (2001). Arm to leg coordination in humans during walking, creeping and swimming activities. *Exp Brain Res* **141,** 375–379.

Weersink JB, Eikelboom C, Dominguez Vega ZT, Maurits NM & de Jong BM (2018). Forward arm extension as a cue for gait initiation in Parkinson's patients. *Mov*

Disord **33,** 1826–1827.

Weersink JB, Gefferie SR, van Laar T, Maurits NM & de Jong BM (2020). Pre-Movement Cortico-Muscular Dynamics Underlying Improved Parkinson Gait Initiation after Instructed Arm Swing. *J Parkinsons Dis* **10,** 1675–1693.

Weersink JB, Maurits NM & de Jong BM (2019). EEG time-frequency analysis provides arguments for arm swing support in human gait control. *Gait Posture* **70,** 71–78.

Yizhar Z, Boulos S, Inbar O & Carmeli E (2009). The effect of restricted arm swing on energy expenditure in healthy men. *Int J Rehabil Res* **32,** 115–123.

Zehr EP, Loadman PM & Hundza SR (2012). Neural control of rhythmic arm cycling after stroke. *J Neurophysiol* **108,** 891–905.

Additional information section

Data availability

Since sharing data in an open-access repository was not included in our participant's consent and therefore compromises our ethical standards, obtained data are only available on request from the corresponding author.

Conflict of interests

The authors report no conflicts of interest

Author contributions

Experiments were performed in the University Medical Center Groningen. Conception and design: J.B.W., B.M.J. and N.M.M. Data acquisition: J.B.W. Analysis and interpretation: J.B.W., B.M.J., N.M.M. and D.M.H. Drafting manuscript: J.B.W., B.M.J. and N.M.M. Revising manuscript: B.M.J., N.M.M. and D.M.H. All authors have read and approved the final version of this manuscript and agree to be accountable for all aspects of the work in ensuring that questions related to the accuracy or integrity of any part of the work are appropriately investigated and resolved. All persons designated as authors qualify for authorship, and all those who qualify for authorship are listed.

Acknowledgements

We would like to thank the patients, their partners and the healthy participants who participated in this study.

Funding

J.W. was supported by an MD/PhD grant from the Junior Scientific Masterclass of the University of Groningen.

Tables

Table 1: Statistical testing forward and reverse connectivity estimates

p-values		TA L	SL	RF L	BF L	TA R	S R	RF R	BF R
DA R	α	0.135	0.030*	0.351	0.526	0.073	0.015*	0.332	0.006*
	β	0.014*	0.218	0.156	0.117	0.052	0.052	0.232	0.010*
	γ	0.191	0.108	0.218	0.067*	0.455	0.351	0.526	0.067
DP R	α	0.037*	0.007*	0.455	0.037*	0.019*	0.009*	0.156	0.008*
	β	0.019*	0.010*	0.117	0.218	0.093	0.004*	0.179	0.006*
	γ	0.279	0.093	0.04*	0.033*	0.391	0.575	0.911	0.030*
DA L	α	0.100	0.156	0.681	0.433	0.052	0.057	0.433	0.370
	β	0.008*	0.191	0.263	0.575	0.794	0.052	0.823	0.601
	γ	0.332	0.550	0.411	0.881	0.455	0.852	0.028*	0.601
DP L	α	0.881	0.502	0.093	0.575	0.093	0.126	0.940	0.765
	β	0.204	0.601	0.279	0.478	0.218	0.033*	0.765	0.550
	γ	0.067	0.765	0.765	0.332	0.167	0.575	0.681	0.765

P-values resulting from the Wilcoxon Signed Rank test that compared the area under the curve for distinct frequency bands between forward (i.e. shoulders to legs) and reverse (i.e. legs to shoulders) connectivity estimation during gait in healthy participants (n=20).

Abbreviations: TA = tibialis anterior, S = soleus, RF = rectus femoris, BF = biceps femoris, DA = deltoideus anterior, DP = deltoideus posterior, L = left, R = right, α = alpha, β = beta, γ = gamma, * = $p<0.05$

Figure legends

Fig 1: Time-dependent intermuscular coherence between upper and lower limb muscles during gait.

Group averaged (n = 20 participants) intermuscular coherence between upper and lower limb muscles across the frequency spectrum (y-axis, 8-70 Hz) during one gait cycle starting at right heel strike (x-axis, time 0ms). Magnitude of coherence is colour coded and indicated using a colour bar on the right. Non-significant values ($p<0.05$) are masked by the darkest blue colour. Vertical lines mark the occurrence of left toe-off (LTO), left heel strike (LHS), right toe-off (RTO) and right heel strike (RHS, time 0), averaged across all participants.

Fig 2. Grand averaged EMG envelopes of upper and lower limb muscles during one gait cycle.

Grand averaged (n= 20) EMG envelopes of all investigated muscles from upper and lower limbs time-warped to the duration of one gait cycle. Vertical solid lines depict moments of heel strike, where dashed vertical lines represent toe-off. EMG-activity on the y-axis is expressed as percentage of the mean activity during one gait cycle.

Fig 3. Time domain estimates for coherence between upper and lower limb muscles during gait

A) Group averaged (n=20) time domain estimates for coherence between upper and lower limb muscles during gait. Dotted horizontal lines depict the upper and lower 95% confidence limits based on the assumption of uncorrelated time series. The significance plots underneath the time estimate plots display coloured squares when time estimates exceeded these 95% confidence limits. B) Theoretical overview of the conduction times for a possible common driver and subcortical and transcortical pathways based on previous literature. 'Arm' and 'leg' represent cortical or spinal representation of the arms and legs. The left plot represents the common driver including the conduction delay of 7ms for arm versus leg muscles (Matamala, 2013), which in figure 3A is

represented by black squares. The right plot represent the theoretical transcortical pathways. The ascending/descending loop with the arm muscles takes > 38ms, where the dotted arrows represent the concept of putative mechanisms of feed forward within the central nervous system and/or feedback from the upper limbs. Combining this with a latency of ±32 ms from the descending pathway to the leg muscles results in a total transcortical latency of >70ms (Nielsen, 1997), which is represented by blue squares in figure 3A. The middle plot represents the subcortical pathways that are proposed to take less time than transcortical pathways and therefore thought to be responsible for the remaining interval of 7-70ms, which are depicted by orange squares in figure 3A.

Fig 4. Zero-lag components of coherence between upper and lower limb muscles during gait

Group averaged (n = 20) zero-lag components of coherence (y-axis) between upper and lower limb muscles during gait across the frequency spectrum (x-axis, 8-70 Hz) are indicated by the solid thick line, where the shaded band depicts the 95% confidence interval. The horizontal dashed line is the upper 95% confidence limit for significant total coherence based on the assumption of uncorrelated time series.

Fig 5. Forward and reverse directed components of coherence between upper and lower limb muscles during gait

Group averaged (n = 20) directed components of coherence (y-axis) between upper and lower limb muscles during gait across the frequency spectrum (x-axis, 8-70 Hz) indicated by the solid thick line, where the shaded band depicts the 95% confidence interval. Blue colours indicate a forward direction where shoulder muscles drive leg muscles, whereas black colours indicate a reverse direction where leg muscles drive shoulder muscles. The horizontal dashed line is the upper 95% confidence limit for significant total coherence based on the assumption of uncorrelated time series. Values in the right upper corner of each muscle combination represent the significant differences between forward and reverse direction connectivity in the distinct frequency bands with corresponding p-values. Abbreviations: α = alpha, β = beta, γ = gamma.

Figures

Fig 1. Time dependent intermuscular coherence between upper and lower limb muscles during gait

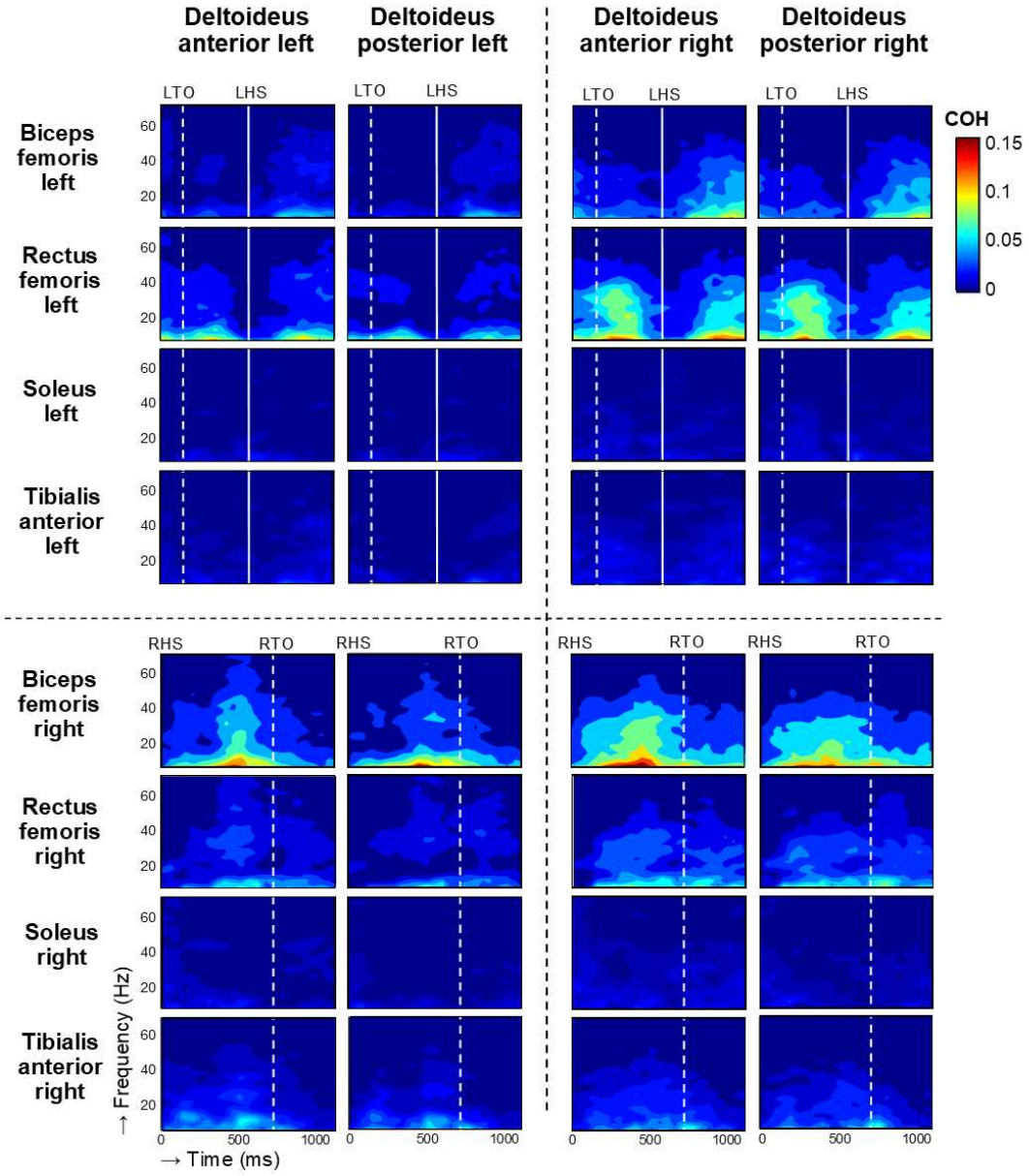

Fig 2. Grand averaged EMG envelopes of upper and lower limb muscles during one gait cycle.

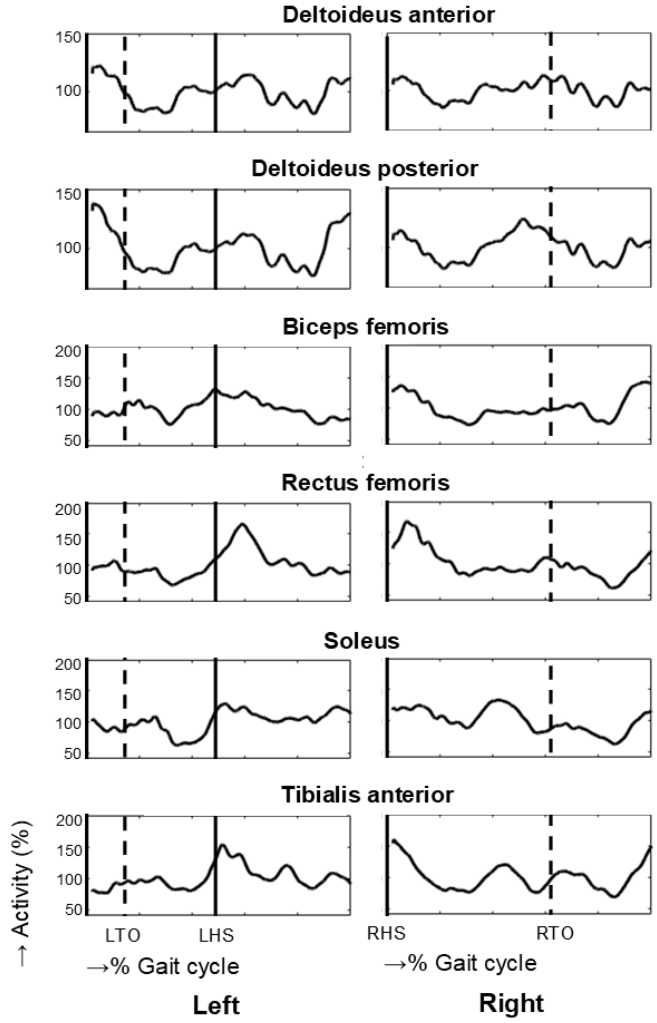

Fig 3. Time domain estimates for coherence between upper and lower limb muscles during gait

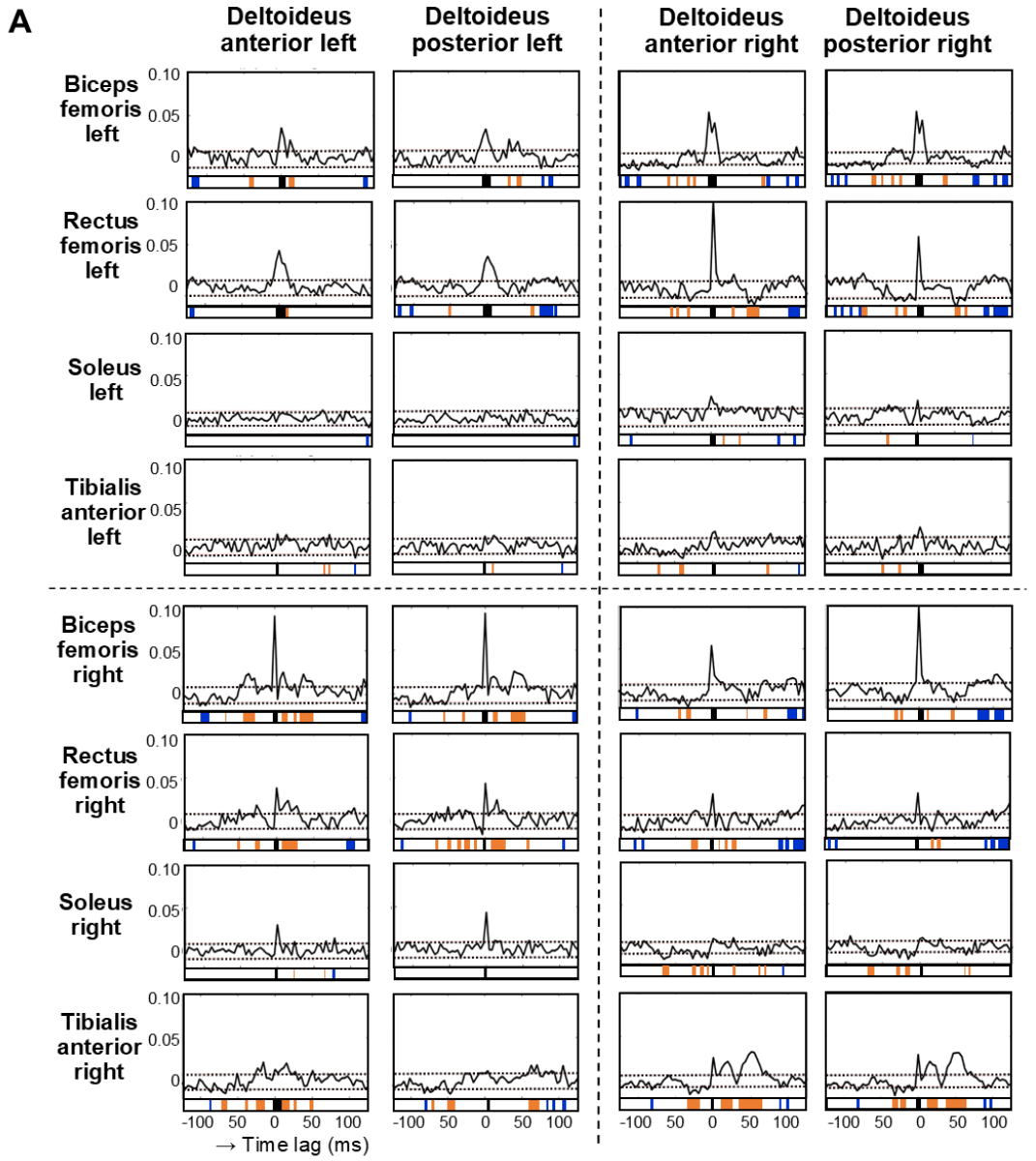

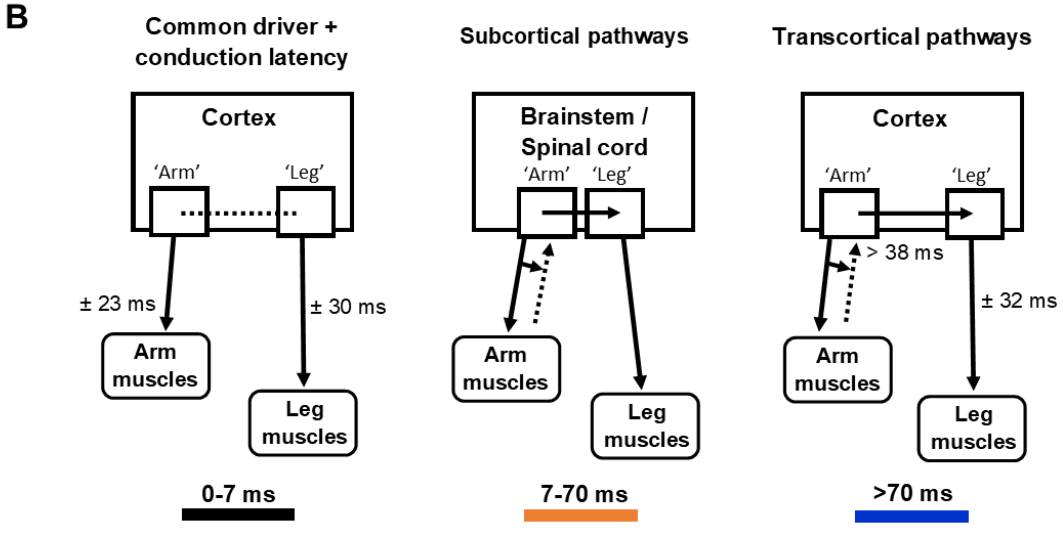

Fig 4. Zero–lag component of coherence between upper and lower limb muscles during gait

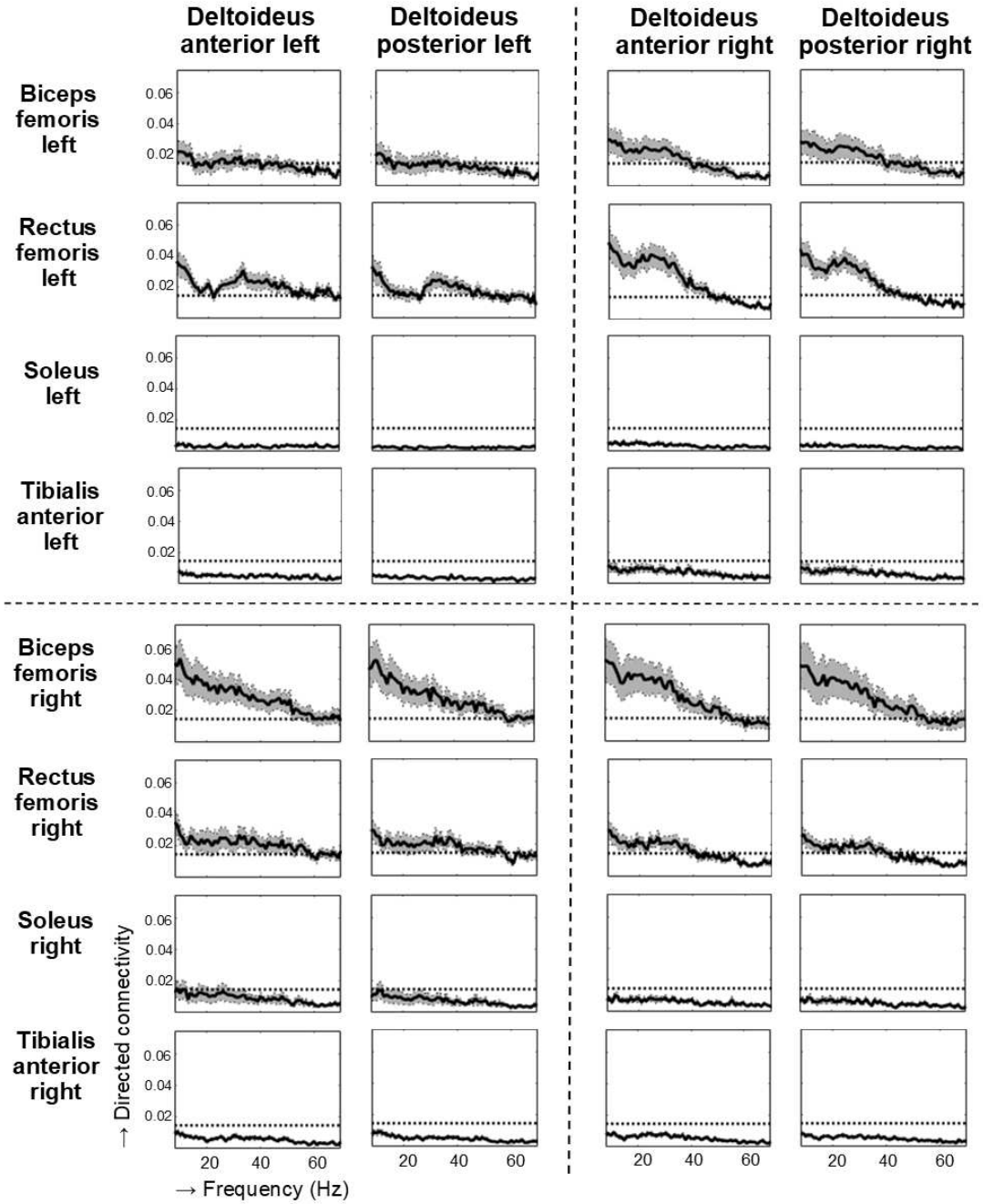

Fig 5. Forward and reverse directed components of coherence between upper and lower limb muscles during gait